Cloud Nowcasting using Artificial Intelligence for Spacecraft Observation Planning

Rens Jan van der Linden[1], Amaury Perrocheau[1], Peter Novák[2], Antonín Komenda[2], Aubrey Dunne[1], David Rijlaarsdam[1]

[1] *Ubotica Technologies, 11 Old Finglas Rd, D11 KXN4, Dublin, Ireland*

[2] *Meandair, Olof Palmestraat 14,2616 LR, Delft, Netherlands*

***Abstract*—Cloud cover is a major challenge in optical satellite imaging, leading to significant data loss and reduced operational efficiency. This study explores the potential of nowcasting-based cloud prediction for spacecraft observation planning, utilizing commercially available cloud forecasts. A proof-of-concept experiment was conducted using Sentinel-2 data, where cloud predictions were interpreted through a logistic function and validated against ground truth cloud masks. The results show that the cloud predictions achieve approximately 90% accuracy at the time of acquisition, decreasing to 75% five hours before observation. These findings highlight the feasibility of integrating nowcasting into observation planning to enhance operational efficiency.**

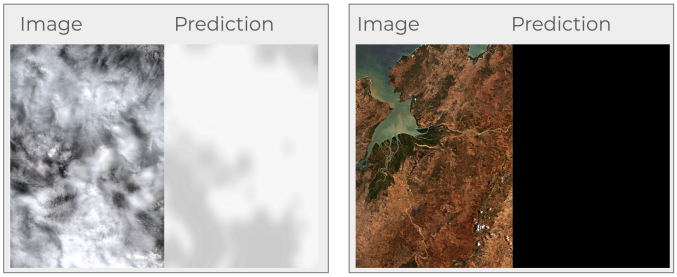

Fig. 1. Image and nowcast prediction for a cloudy image (left) and a clear image (right)

I. Introduction

The operational efficiency and data quality of optical satellite imaging are highly dependent on atmospheric conditions, with cloud cover being one of the most significant challenges. Optical satellites cannot typically capture imagery through clouds, leading to substantial data loss. This interference can range from complete occlusion to partial distortion from, for example, cloud shadows, which compromises the accuracy of satellite imagery for various applications. During NASA's MODIS mission, it was reported that approximately 67% of captured images were classified as cloudy, illustrating the impact of cloud cover on satellite observation [1]. Traditional methods for minimizing cloud interference often rely on the generation of cloud masks on the ground to filter out cloud-affected pixels [2], [3]. Although these cloud masks effectively filter unusable portions of an image, they do not prevent the unnecessary use of bandwidth and power required to capture and transmit the acquisition.

To address this, Giuffrida et al. proposed a Neural Network designed to run directly on the satellite, identifying and excluding areas affected by clouds before downlinking images [4]. This approach can even be incorporated into adaptive scheduling models, dynamically altering the observation plan based on the detected clouds onboard [5].

However, if the cloud cover was known in advance, satellite resources could be scheduled even more efficiently. Wang et al. [6] underscored that uncertainty in cloud cover directly impacts the scheduling effectiveness of agile spacecraft, as cloud-free imaging opportunities become critical to efficient task planning. Similarly, Lin et al. [7] developed a sophisticated scheduling system, demonstrating how incorporating cloud cover predictions could optimize satellite scheduling by balancing factors like power constraints and data collected. This is especially relevant for scheduling multi-modal constellations, where diverse sensor types such as optical and Synthetic Aperture Radar (SAR) can complement each other. Unlike optical sensors, SAR technology can capture acquisitions through cloud cover. However, SAR satellites are typically more limited in observational duty cycle. Therefore, effective cloud prediction enables a more strategic allocation of tasks across a multi-modal constellation, optimizing which satellite should be used for a given observation [8].

Nowcasting is a short-term weather forecasting technique which extrapolates available current weather data to create a forecast for the coming hours. The commercially available technology (the Meandair Nowcasting Weather Engine) used in this paper leverages AI to generate high resolution, near real-time predictions of cloud cover. This data can be used to inform observational planning of Earth Observation (EO) spacecraft. Figure 1 illustrates the potential of nowcasting for planning spacecraft observations, showcasing predicted and actual cloud cover under both clear and cloudy conditions.

In recent years, various studies have demonstrated the potential of nowcasting to support satellite operations. For instance, Roussel et al. adapted cloud prediction models originally used for photovoltaic energy applications to satellite Earth observation, achieving notable accuracy in their forecasting results, with a true positive rate of 81.6% and a false positive rate of 10.1% at 90 minutes before the observation [9]. Yi Gu et al., developed a dynamic scheduling approach that integrates predictive recurrent neural networks (PredRNN) to anticipate cloud coverage. Their results show that predictive scheduling models can improve both the efficiency and accuracy of task planning compared to conventional methods. However, their

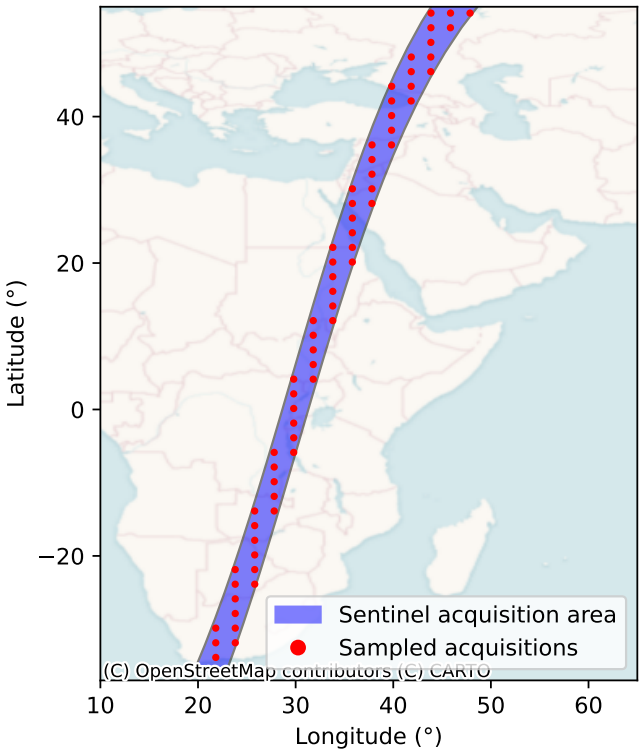

Fig. 2. Example of sampled acquisition

study was limited to point targets and did not address broader areas of interest [10].

In this work we show that these predictions provide a good prediction of local cloud levels, by cross-referencing nowcasting predictions with Sentinel-2 acquisitions. We argue that these predictions can be used in two ways: 1) to inform planning to predict if an acquisition will be affected by clouds before capture and 2) to re-plan failed acquisitions by determining if an acquisition was affected by clouds before receiving data on ground. This solution complements existing on-board cloud detection solutions and increases the efficiency of EO spacecraft.

II. Methodology

The weather predictions used in this work were provided through an API to the Meandair Nowcasting Weather Engine [11], which is commercially available. To verify the performance of the cloud predictions provided, a proof of concept has been devised using Sentinel-2.

A. Dataset collection

Upcoming Sentinel-2 acquisition plans are available for download from the Copernicus website [12]. A typical acquisition stretches from one pole to the other. Because the scale of the observation affects accuracy, samples were taken at the scale of CubeSat acquisitions, which was set at a 20x30 km area. Figure 2 shows an example of the sampling of a Sentinel-2 acquisition.

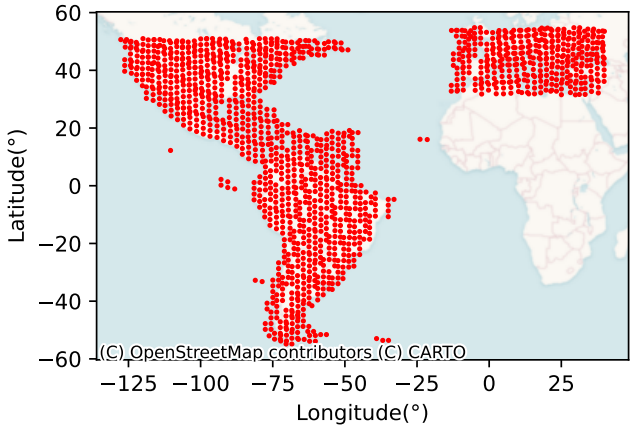

Fig. 3. Coverage of the test set

Because a Sentinel-2 acquisition can last for up to five hours, the exact time at which each sample is captured depends on its position within the acquisition. To accurately determine the acquisition time for each sample, a linear interpolation was performed. This calculation was based on the start time and duration of the Sentinel-2 acquisition, as well as the start and end latitudes. Using the center latitude of each sample, its corresponding acquisition time was interpolated. The interpolated time, $t_{\text{interpolated}}$, is calculated by the following equation:

$$t_{\text{interpolated}} = t_{\text{start}} + \left(\frac{\text{lat} - \text{lat}_{\text{min}}}{\text{lat}_{\text{max}} - \text{lat}_{\text{min}}} \right) \cdot \text{duration} \qquad (1)$$

where $t_{\text{interpolated}}$ represents the interpolated timestamp, t_{start} is the starting time of the acquisition, lat is the latitude of the sample, lat_{min} and lat_{max} are the minimum and maximum latitudes of the acquisition, and duration is the total duration of the acquisition in milliseconds. To gather cloud predictions for each of these samples, nowcasting predictions were collected every 10 minutes, starting from 5 hours prior to the acquisition time. Finally, to obtain ground truth against which to compare the cloud predictions, the actual images and cloud masks were downloaded from Sentinel Hub [13] which uses its in-house model, S2Cloudless, to extract the cloud masks [14].

The data was gathered for one week, starting on November 19, 2024. This dataset was split into a tuning set for the first day and a test set for the remaining six days. This resulted in 312 samples in the tuning set and 1476 samples in the test set. The coverage of the test set is shown in Figure 3.

B. Prediction interpretation

The nowcasting predictions have pixel values between 0 and 100, representing cloud opacity as a percentage. To convert these opacity values into probabilities of cloud cover, a logistic function is applied. The formula to convert the cloud opacity to a probability is the following:

$$f(x) = \frac{1}{1 + e^{-k(x - x_0)}} \qquad (2)$$

Where k is the growth rate and x_0 is the center of the curve. The cloud cover probability for the image is then the

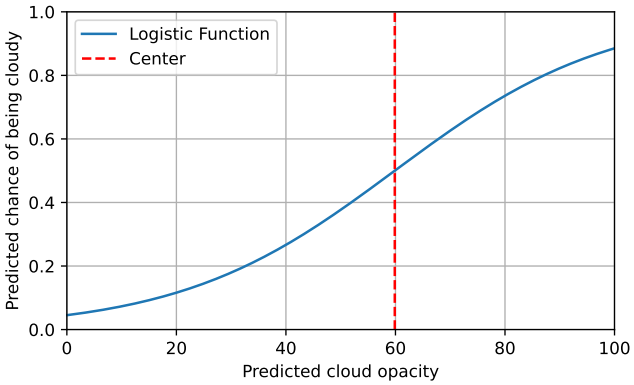

Fig. 4. Plot of the tuned sigmoid

average of the probabilities over all pixels. To tune the logistic function, the root mean squared error (RMSE) is computed between the cloud cover probabilities in the predicted maps and the actual cloud masks. The differential evolution algorithm was used to find the parameters of the logistic function that minimize the RMSE [15]. To obtain a logistic function suitable for use across all cloud cover ranges, the tuning dataset was balanced using 25% bins, resulting in 28 images per bin for 0%–25%, 25%–50%, 50%–75%, and 75%–100%. The tuned logistic function is shown in Figure 4.

C. Metrics

The metrics of interest vary depending on the use case of the predictions. The metrics used in this experiment are accuracy, precision, and sensitivity. Accuracy indicates overall performance, precision reflects the absence of false positives, and sensitivity reflects the absence of false negatives. Accuracy is defined as follows:

$$\text{Accuracy} = \frac{\text{TP} + \text{TN}}{\text{TP} + \text{TN} + \text{FP} + \text{FN}} \tag{3}$$

where TP represents true positives, TN represents true negatives, FP represents false positives, and FN represents false negatives. Accuracy is used to assess overall performance.

For the rescheduling use case, where a captured but not received acquisition is predicted to be cloudy, it is important to minimize both false positives and false negatives. Predicting an image to be cloudy when it is actually clear (a false positive) results in wasted satellite resources. The metric used to evaluate this is precision:

$$\text{Precision} = \frac{\text{TP}}{\text{TP} + \text{FP}} \tag{4}$$

When considering the use case of canceling acquisitions, the metric of sensitivity also becomes important:

$$\text{Sensitivity} = \frac{\text{TP}}{\text{TP} + \text{FN}} \tag{5}$$

This metric is high when the number of false negatives is low. A low number of false negatives means that acquisitions are canceled primarily when they are truly cloudy.

D. Experimental Setup

For the test dataset, nowcasting maps and actual cloud masks were collected and analyzed. A maximum cloud cover threshold was applied, with tests conducted at 20%, 40%, and 60% thresholds. Based on these thresholds, images were classified as either cloudy or clear. This classification was performed separately for both the nowcast predictions and the actual cloud masks. The classification results were then compared to evaluate the agreement between predicted and actual cloud cover. Finally, the metrics described above were calculated to assess performance.

III. Results

Figure 5 shows the evolution of the nowcast performance over the full 5 hour prediction window. Initially, the model achieves high accuracy, starting at nearly 90%. As expected, over the 5-hour period, this accuracy gradually decreases to around 75%. A similar trend is observed with precision. Sensitivity begins at 95%, reflecting a low occurrence of false negatives at the time of acquisition.

The performance decline over time is less significant when predicting under lower cloud cover thresholds, compared to higher cloud cover thresholds. This suggests that cloud cover thresholds influence the predictive reliability of nowcast over extended durations. The overall result confirms the feasibility of cloud cover prediction for satellite acquisitions. It allows for the prediction of an image being cloudy at the time of acquisition and even 5 hours before the acquisition with an accuracy of 75%. The high initial accuracy suggests that the interpretation of the cloud predictions is done correctly, and that the decrease is due to nowcasting becoming less precise as the time until acquisition increases.

IV. Conclusions

This paper proves the feasibility of using cloud predictions to accurately determine whether an acquisition will be cloudy before being taken, and to accurately determine if an acquisition was cloudy directly after being taken but before receiving data on ground. This capability allows for dynamic observation schedule adjustments, ultimately increasing the amount of valuable data generated by Earth Observation spacecraft.

References

[1] M. D. King, S. Platnick, W. P. Menzel, S. A. Ackerman, and P. A. Hubanks, "Spatial and temporal distribution of clouds observed by MODIS onboard the terra and aqua satellites," *IEEE Transactions on Geoscience and Remote Sensing*, vol. 51, no. 7, pp. 3826–3852, 2013.

[2] L. Baetens, C. Desjardins, and O. Hagolle, "Validation of copernicus sentinel-2 cloud masks obtained from MAJA, sen2cor, and FMask processors using reference cloud masks generated with a supervised active learning procedure," *Remote Sensing*, vol. 11, no. 4, p. 433, 2019.

[3] S. Skakun, J. Wevers, C. Brockmann, G. Doxani, M. Aleksandrov, M. Batič, D. Frantz, F. Gascon, L. Gómez-Chova, O. Hagolle, D. López-Puigdollers, J. Louis, M. Lubej, G. Mateo-García, J. Osman, D. Peressutti, B. Pflug, J. Puc, R. Richter, J.-C. Roger, P. Scaramuzza, E. Vermote, N. Vesel, A. Zupanc, and L. Žust, "Cloud mask intercomparison eXercise (CMIX): An evaluation of cloud masking algorithms for landsat 8 and sentinel-2," *Remote Sensing of Environment*, vol. 274, p. 112990, 2022.

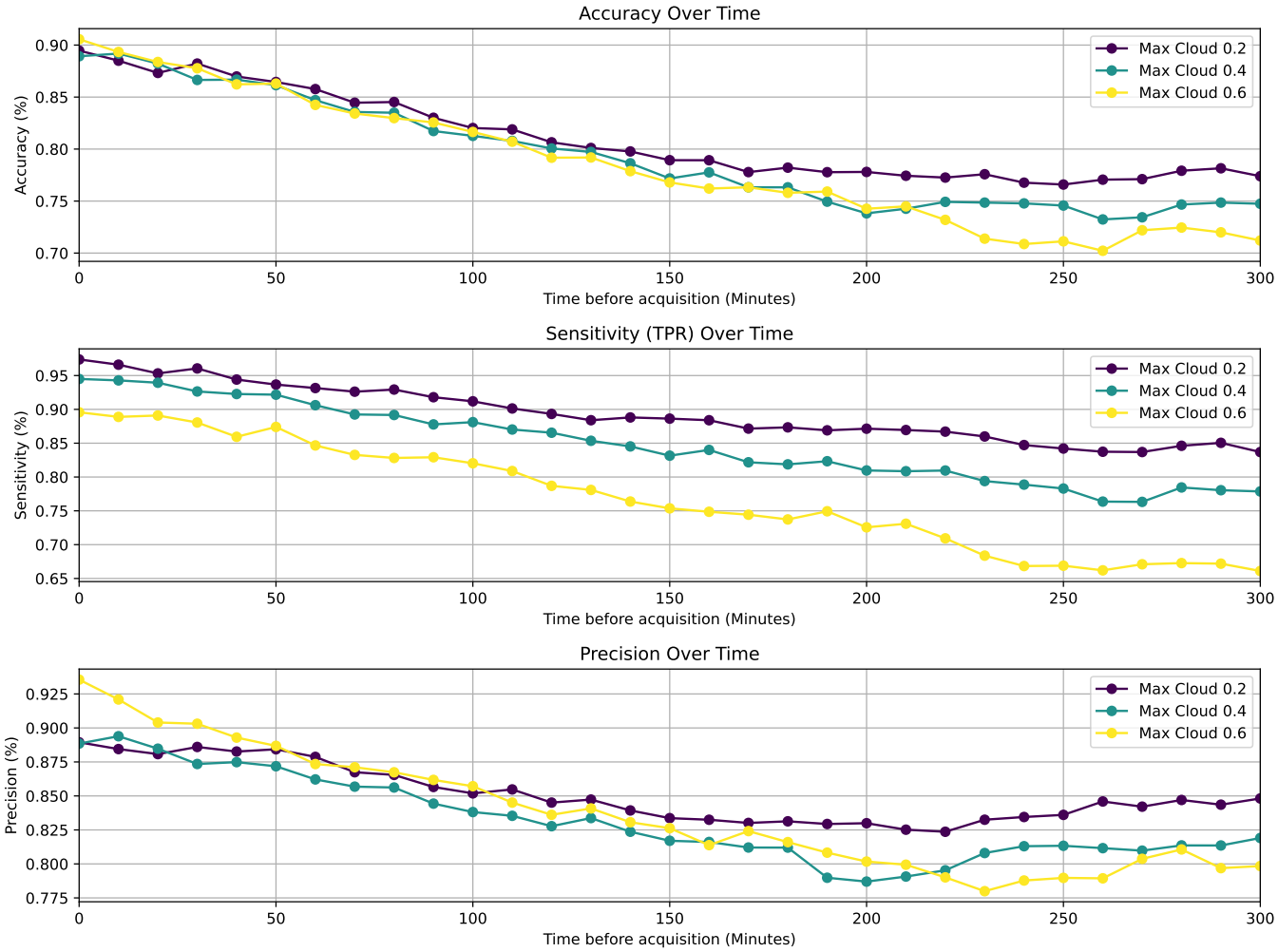

Fig. 5. Evolution of nowcast performance over time. Max Cloud indicated cloud cover thresholds.

[4] G. Giuffrida, L. Fanucci, G. Meoni, M. Batič, L. Buckley, A. Dunne, C. van Dijk, M. Esposito, J. Hefele, N. Vercruyssen, G. Furano, M. Pastena, and J. Aschbacher, "The ϕ-sat-1 mission: The first on-board deep neural network demonstrator for satellite earth observation," *IEEE Transactions on Geoscience and Remote Sensing*, vol. 60, pp. 1–14, 2022.

[5] S. Chien, R. Sherwood, D. Tran, B. Cichy, G. Rabideau, R. Castano, A. Davies, R. Lee, D. Mandl, S. Frye *et al.*, "The eo-1 autonomous science agent," in *Proceedings of the Third International Joint Conference on Autonomous Agents and Multiagent Systems-Volume 1*, 2004, pp. 420–427.

[6] X. Wang, G. Wu, L. Xing, and W. Pedrycz, "Agile earth observation satellite scheduling over 20 years: Formulations, methods, and future directions," *IEEE Systems Journal*, vol. 15, no. 3, pp. 3881–3892, 2020.

[7] W.-C. Lin, D.-Y. Liao, C.-Y. Liu, and Y.-Y. Lee, "Daily imaging scheduling of an earth observation satellite," *IEEE Transactions on Systems, Man, and Cybernetics-Part A: Systems and Humans*, vol. 35, no. 2, pp. 213–223, 2005.

[8] A. Globus, J. Crawford, J. Lohn, R. Morris, and D. Clancy, "Scheduling earth observing fleets using evolutionary algorithms: Problem description and approach," 2002, NTRS Author Affiliations: NASA Ames Research Center, NTRS Document ID: 20020091594 NTRS Research Center: Ames Research Center (ARC). [Online]. Available: https://ntrs.nasa.gov/citations/20020091594

[9] G. Roussel, M. Turpin, Y. Bardout, and G. Jubelin, "Adaptation of short-term cloud forecasting to global scale and evaluation of its contribution to earth observing satellite planning," *IEEE Journal of Selected Topics in Applied Earth Observations and Remote Sensing*, vol. 14, pp. 12 524–12 535, 2021.

[10] Y. Gu, C. Han, Y. Chen, and W. W. Xing, "Mission replanning for multiple agile earth observation satellites based on cloud coverage forecasting," *IEEE Journal of Selected Topics in Applied Earth Observations and Remote Sensing*, vol. 15, pp. 594–608, 2021.

[11] Meandair nowcasting weather engine. Meandair BV. [Online]. Available: https://www.meandair.com/

[12] Sentinel-2 acquisition plans. Copernicus - Sentinel Programme. [Online]. Available: https://sentinels.copernicus.eu/web/sentinel/copernicus/sentinel-2/acquisition-plans

[13] Sentinel hub. Sinergise Solutions. [Online]. Available: https://www.sentinel-hub.com

[14] S. Skakun, J. Wevers, C. Brockmann, G. Doxani, M. Aleksandrov, M. Batič, D. Frantz, F. Gascon, L. Gómez-Chova, O. Hagolle *et al.*, "Cloud mask intercomparison exercise (cmix): An evaluation of cloud masking algorithms for landsat 8 and sentinel-2," *Remote Sensing of Environment*, vol. 274, p. 112990, 2022.

[15] R. Storn and K. Price, "Differential evolution–a simple and efficient heuristic for global optimization over continuous spaces," *Journal of global optimization*, vol. 11, pp. 341–359, 1997.